

Calculating V-1000 Core Model With Serpent 2 - HEXTRAN Code Sequence

Ville Sahlberg,*

*VTT Technical Research Centre of Finland, Espoo, Finland
ville.sahlberg@vtt.fi

Abstract - Continuous-energy Monte Carlo reactor physics code Serpent 2 was used to model the critical steady state conditions measured in V-1000 zero-power critical facility at the present day NRC "Kurchatov Institute", Moscow in 1990-1992. The Serpent 2 results were compared to measurements and Serpent 2 was used to generate group constants and albedo boundary conditions for two-group nodal diffusion reactor dynamics code HEXTRAN. The results of a HEXTRAN calculation of the steady state were compared to Serpent 2. Initial 3D Serpent 2 calculation produced an effective multiplication factor of $k_{eff} = 1.01480$ for the critical steady state. Subsequent calculations showed that adding the stainless steel spacer grids of the V-1000 core to the Serpent 2 model lowered this overestimation by 660 pcm. Furthermore, it was found that the soluble boron concentration of the steady state has the potential to shift the effective multiplication factor by up to 577 pcm while still staying within its experimental accuracy. When the soluble boron concentration was set to the highest allowable concentration within its experimental accuracy and the spacer grids were taken into account, Serpent 2 produced a $k_{eff} = 1.00243$ for the critical steady state. HEXTRAN produced an effective multiplication factor within 521 pcm of the corresponding full core Serpent 2 calculation. There was a tilt in the HEXTRAN solution relative to Serpent 2 such that the relative powers in the middle of the core were significantly underestimated.

I. INTRODUCTION

The validation of nodal codes has relied on diffusion benchmarks and comparisons to measurements for most of the history of nodal calculations. While comparison to measurements provides an important view on the usefulness of the calculation chain, it is oftentimes a limited resource for analysing the nodal solver. This is both due to the practical difficulties in taking all relevant parameters of a real-world problem into account as well as due to possible experimental uncertainties of the measurements. Continuous-energy Monte Carlo reactor physics code Serpent 2 enables the generation of homogenized group constants and calculation of 3D reference solutions with the same code [1]. This enables the generation of test cases at will, not limited by available experimental data.

In this work, a zero power critical steady state of the V-1000 zero-power critical facility [2] at NRC "Kurchatov Institute" is used to analyze Serpent 2 - HEXTRAN [3] calculation chain and Serpent 2 full core calculation results. Serpent 2 is used to generate group constants and albedo boundary conditions for the nodal reactor dynamics code HEXTRAN and the Serpent 2 and HEXTRAN solutions are compared to ensure the successful implementation of the Serpent 2 - HEXTRAN code sequence. In addition, the Serpent 2 results are compared to measurements of the steady state carried out at the former I.V. Kurchatov Institute of Atomic Energy / Russian Scientific Centre in 1990-1992 [2].

The case has been previously calculated by several institutions with the codes HEXTRAN, KIKO3D [4], DYN3D [5] and BIPR-8 [6] in EU FP5 programme [7]. The homogenized parameters for these previous cases were generated by codes WIMS8 [8], CASMO-4 [9], HELIOS-1.5 [10], TVS-M [11] and NESSEL-4 [12]. The albedo boundary conditions for the previous calculations were generated by Dr. P.T. Petkov using the MARIKO 32-group transport code [13, 14].

II. THE V-1000 FACILITY

The V-1000 zero-power critical facility (ZPCF V-1000) is a full-scale model of a VVER-1000 core. The core consists of 163 VVER-1000 fuel assemblies with 312 fuel rods each and a lattice pitch of 23.6 cm. The core has 61 finger-type control rod clusters with 18 absorber rods each. The criticality of the core is controlled by adjusting the moderator level in the core and the active length of the core is 353 cm.

The core is surrounded by solid stainless steel reflector (core baffle) with vertical cylindrical holes labeled A-, B- and C-type holes at several positions. The six A-type holes have a diameter of 95 mm and are located at the natural corners of the hexagonal core. The six B-type holes are shifted two assemblies counter-clockwise from the A-type holes and have a diameter of 75 mm. The 12 C-type holes are located near the south-western face of the core and have a diameter of 70 mm. All of the C-type holes are plugged with stainless steel bolts with a diameter of 65 mm. The A- and B-type holes and the ring-shaped gaps around the stainless steel bolts in C-type holes are filled with moderator up to the moderator level of the core. The eastern and the western B-type holes have KNK-56 ionization chambers inserted. In addition, there are gaps between the fuel assembly faces and the core baffle which vary between 1.7 and 5.4 mm (± 0.2 mm measurement accuracy [15]) and the layer between the core baffle and the reactor tank is also filled with moderator. The radial arrangement is shown in Fig. 1. The core has a startup load with four different fuel assembly types which are given in Table I. The notable deviation from the typical VVER-1000 assemblies is that the V-1000 core utilizes boron as burnable absorber instead of gadolinium. In addition, the spacer grids in the V-1000 are composed of stainless steel.

The critical steady state analyzed in this work had all control rods withdrawn from the core, moderator level 266.8

Table I. Properties of the fuel assemblies

Assembly type	Uranium enrichment	Additional properties
A	1.6% [2]	
C	3.0% [2]	
F	4.4/3.6% [2]	4.4% profiled with 3.6%, has boron burnable absorber pins [2]
I	4.4% [2]	Has boron burnable absorber pins [2]

cm from the bottom of the active fuel area and boron acid concentration of 8.68 g/l (± 0.3 g/l experimental accuracy). The moderator and fuel temperatures were 15.2 C. The experimental measurements were carried out at KI by placing partial-length (50 cm) fuel rods into the guide tubes in the middle of the assemblies with the axial middle points of the detector rods 120 cm above the bottom of the active fuel area and irradiating them for 20 minutes at critical state. The irradiated fuel pins were afterwards removed from the core and their gamma activity was measured. The measurement results were normalized against the measurements from the detector rod from assembly #27. The enrichments of the detector rods corresponded to the enrichment level of the fuel pins surrounding the central tube. The relative power measurements have measurement accuracies of 3% for assemblies with relative powers higher than 0.1 and 10% for assemblies with relative powers less than 0.1. [2]

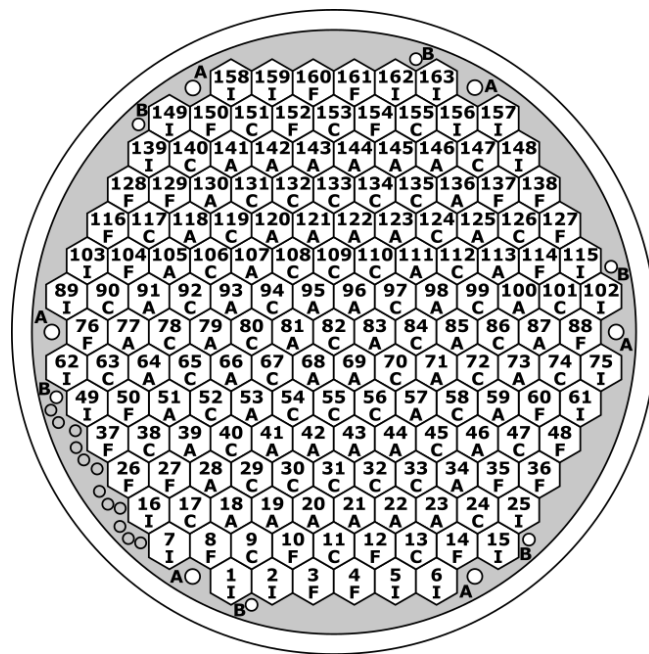


Figure 1. The radial geometry of the core of the V-1000 facility. Assembly types and numbers and the A- and B-type holes are marked to the illustration. [16]

III. CALCULATIONS

For the analysis of the case the following calculations were made with Serpent 2 and HEXTRAN:

- Group constant calculations with Serpent 2
- Albedo calculations with Serpent 2
- Three 3D full core calculations with Serpent 2
- Full core calculation with HEXTRAN

1. Group constant calculations

The group constants were calculated with 2D single-assembly Serpent 2 calculations for the four assembly types for conditions below the moderator level in the core. Separate group constants were calculated for fuel areas with and without detector rods. The group constants for the dry parts of the assemblies were not calculated. Instead group constants generated previously with CASMO-4 were used for the dry parts. The impact of this on the results was considered negligible, as the axial flux vanishes quickly above the moderator level. This simplified the group constant calculation, as in dry geometry the neutron population for solving thermal group's constants was extremely low in Serpent 2. Proper group constant generation for the dry parts would have required the use of the 3D homogenization features of Serpent 2.

Infinite lattice spectrum was used for the group constant generation in addition to reflective boundary conditions. The diffusion coefficients were calculated using the cumulative migration method [17]. The cross section libraries for Serpent 2 were based on ENDFB-7.1. The cross sections were Doppler broadened to the steady state temperatures from 0 Kelvin cross sections.

2. Albedo calculations

As the HEXTRAN code utilizes albedo boundary conditions immediately outside the active fuel area of the core, rigorous generation of the albedos is especially important. In this work, three radial albedos were calculated for the core with Serpent 2 in 2D geometry to take into account two-dimensional leakage effects. The rest of the radial albedos and the axial albedos were taken from Dr. Petkov's work [13, 14]. One of the albedo surfaces used in this work is presented in Fig. 2. The radial albedos generated with Serpent 2 were located at the natural corners of the core (on top of the A-type holes), two assembly faces counterclockwise from the natural corners (on top of the B-type holes) and at the assembly face between these two. The albedo boundary conditions included cross-terms from fast to thermal group and vice versa.

3. Serpent 2 full core calculations

Three 3D full core Serpent 2 calculations of the V-1000 core were performed. The core was modeled from 80 cm below the active fuel area to the top of the active fuel area. Geometry above the fuel was not considered as the flux vanished quickly above the moderator level. The geometry below

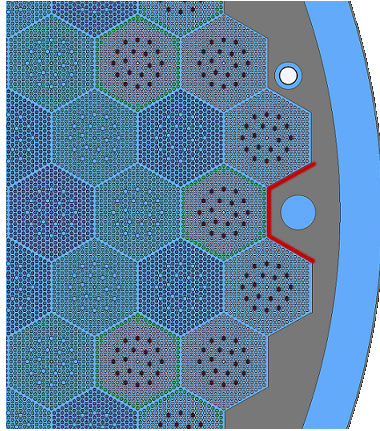


Figure 2. The 2D geometry used for the generation of an albedo block near one of the A -type holes. The red line represents the albedo surface.

the core was modelled as blocks of homogenized areas with differing water/steel ratios. Black boundary conditions were used at the axial boundaries of the model. Radially, the core was modelled to the outer surface of the moderator vessel. Black boundary conditions were used at the radial boundary as well. The full core Serpent 2 model included the A-, B- and C-type holes in the core baffle, the two KNK-56 detectors as well as the moderator in the holes. A combined flux and fission power meshplot of the core at the axial level of the detector rods is presented in Fig. 3.

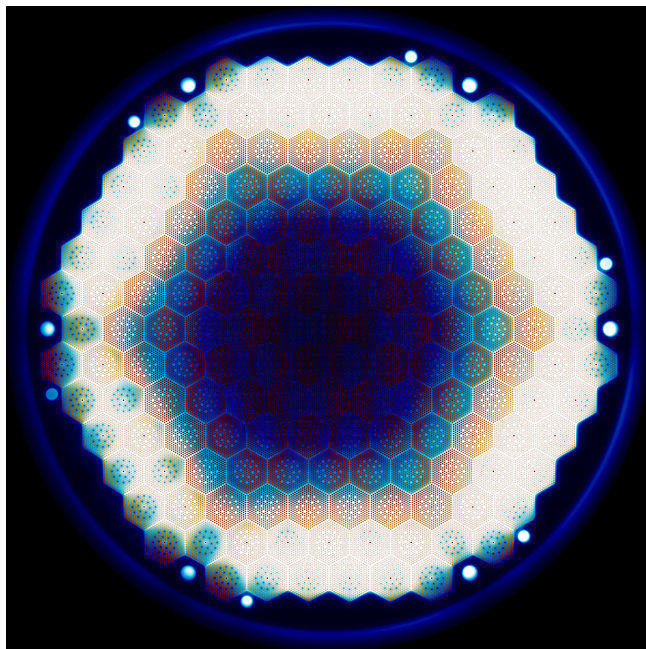


Figure 3. 2D mesh plot of the V-1000 core at the axial level of the detector rods. Cool colors represent thermal flux magnitude and warm colors represent relative fission power.

During the work it was found out the gaps between the core baffle and the fuel assemblies were measured twice at

the present-day NRC “Kurchatov Institute”. The gaps from the first set of measurements provided results which differed significantly from the measurements. Due to difficulties obtaining the second set of measurements, the gaps between the fuel assemblies and the core baffle were solved from past albedo calculations from Dr. Petkov, as the gap widths were listed unambiguously in Dr. Petkov’s work. It is worth noting the measurements of the first pass have an accuracy of ± 1 mm and the accuracy of the second pass is ± 0.2 mm. However, the measurements of the first and second pass differ by quantities larger than these limits. The full core Serpent 2 model was constructed according to the measurements of the second measurement pass. It was also brought to the author’s knowledge that V-1000 had difficulties with the bending of the fuel assemblies, which could affect the gap widths [15].

The three calculations differed so that the first calculation did not incorporate spacer grids in the 3D model. In the other two the spacers grids below the moderator surface were modelled explicitly and spacer grids above the moderator surface were not modelled. In addition, the calculation without spacer grids used the measured boron concentration of 8.68 g/l. The calculations with spacer grids used boron concentrations of 8.68 g/l and 8.98 g/l, which corresponded to the measured concentration and the highest possible concentration within the experimental error. The differences between the calculations are presented in Table II.

Table II. The varied properties of the Serpent 2 calculations

	C_{Boron} (g/l)	Spacer grids
#1	8.68	Not modelled
#2	8.68	Modelled below the moderator surface
#3	8.98	Modelled below the moderator surface

The relative power densities of all fuel pins in the core for all nodes corresponding to the nodalization of the core in HEXTRAN were calculated by Serpent 2. This included directly calculated rod-wise powers of the detector rods in the model. Each of the calculations used 2.5 million neutron histories for each cycle for 50000 active cycles and 1500 inactive cycles for fission source convergence. The full core calculations took approximately a total of 33.9 days on twenty 3000 MHz Intel Xeon CPUs.

4. HEXTRAN calculation

HEXTRAN solves time-dependent two-group diffusion equations by diagonalizing the diffusion matrix and solving the flux eigenmodes. HEXTRAN separates axial and radial flux solutions inside the nodes and uses a third degree polynomial flux expansion for the axial direction and trivariate third degree polynomial flux expansion for the radial direction.

The HEXTRAN calculation used group constants from Serpent 2, with the exception of the dry fuel areas. The group constants for the dry fuel were taken from CASMO-4 calculations. The calculation used albedo boundary conditions from Dr. Petkov as well as from the three Serpent 2 albedo calculations. The spacer grids were not modelled in HEXTRAN.

This was done as the diffusion model in HEXTRAN does not converge to the exact diffusion solution at the limit of very small nodes. This caused unnecessary inaccuracies when using 2 cm axial nodes for the spacers. The total core power was set to 100 W and the time step length was set to zero to model zero-power critical steady state. The HEXTRAN calculation of the critical steady state took approximately 0.29 seconds on a single core of a 2992 MHz Intel Xeon CPU.

IV. CALCULATION RESULTS

1. Comparison of Serpent 2 full core calculations and measurements

All three of the full core Serpent 2 calculations overestimated the effective multiplication factor of the system significantly. The calculation #1 produced a $k_{eff} = 1.01480$ for the critical steady state, and the calculations #2 and #3 provided effective multiplication factors of 1.00820 and 1.00243. The statistical uncertainty of these values was 1.8×10^{-6} for all three cases. In this work statistical uncertainty is defined as the sample standard deviation divided by the sample mean. These results indicate the worth of including the spacer grids in the model to be 660 pcm and the upper limit to the reactivity worth of the uncertainty in the boron concentration to be roughly 600 pcm. The relative differences between the detector rod powers from Serpent 2 calculation #3 and the measurements are presented in Fig. 4. The statistical uncertainty of the relative powers of the detector rods were between 1 to 3 % for most of the detector rods in all of the Serpent 2 calculations.

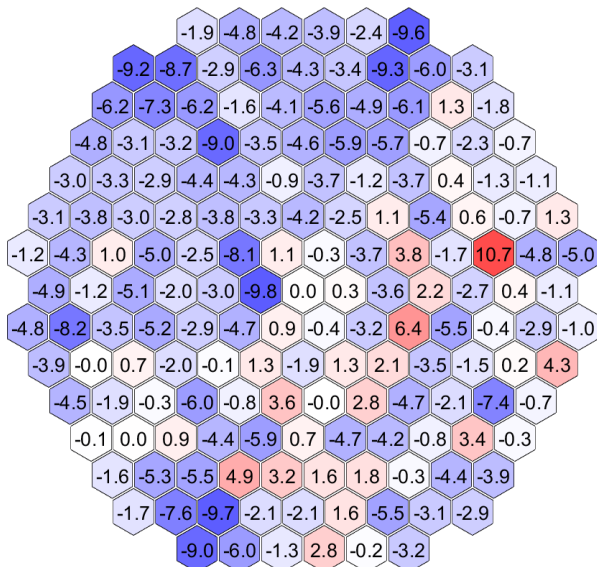


Figure 4. The relative differences in percents between the relative detector rod powers from the full core Serpent 2 calculation #2 and the measurements.

The measured significant tilt in the relative power from the lower left to the upper right of the core was reproduced in all three Serpent 2 calculations. The comparison of the relative detector rod powers from the Serpent 2 calculations and the measurements are presented in Table III. “RMS” is the root

mean square between the relative detector rod powers from Serpent 2 and the measurements, the “Sum” is the percentage of the relative detector rod powers from Serpent 2 which are within the sum of the statistical and experimental uncertainties of the results and measurements, “Quadrature” is the percentage of the relative detector rod powers from Serpent 2 which are within the quadrature of the statistical and experimental uncertainties of the results and measurements and “Range of differences” contains the largest under- and overestimations of the individual relative detector rod powers from Serpent 2 relative to the measurements. The relative differences in the relative powers of the detector rods for which the difference exceeded the sum of the statistical and experimental uncertainty are presented in Fig. 5 for the Serpent 2 calculation #3.

Table III. The 3D Serpent 2 calculation results

	#1	#2	#3
k_{eff}	1.01480	1.00820	1.00243
RMS	4.92×10^{-2}	4.67×10^{-2}	4.15×10^{-2}
Sum (%)	80.98	82.82	88.96
Quadrature (%)	61.35	66.26	67.48
Range of differences (%)	-11.3 +12.7	-11.0 +11.5	-9.8 +10.7

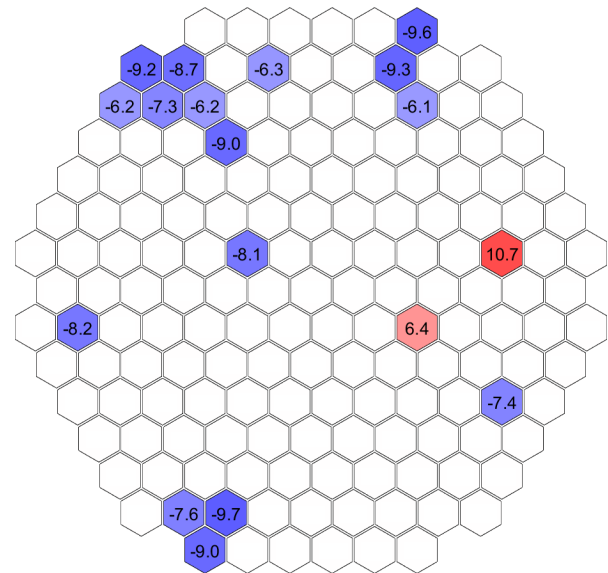


Figure 5. The filtered relative differences in percents between the relative detector rod powers from the full core Serpent 2 calculation #3 and the measurements.

2. Comparison of the Serpent 2 full core calculation #1 and HEXTRAN calculation

The Serpent 2 calculation #1 was chosen for comparison, as then the models in HEXTRAN and Serpent 2 corresponded

to each other. The node-wise HEXTRAN and Serpent 2 results were compared for the nodes in the same axial layer as the detector rods. The largest differences between the node-wise relative powers of HEXTRAN and Serpent 2 were -19.4% and +6.4%. The HEXTRAN calculation produced an effective multiplication factor of $k_{eff} = 1.02001$, within 521 pcm of the Serpent 2 result. The differences between the node-wise relative powers of HEXTRAN and Serpent 2 at the axial level of the detector rods are presented in Fig. 6.

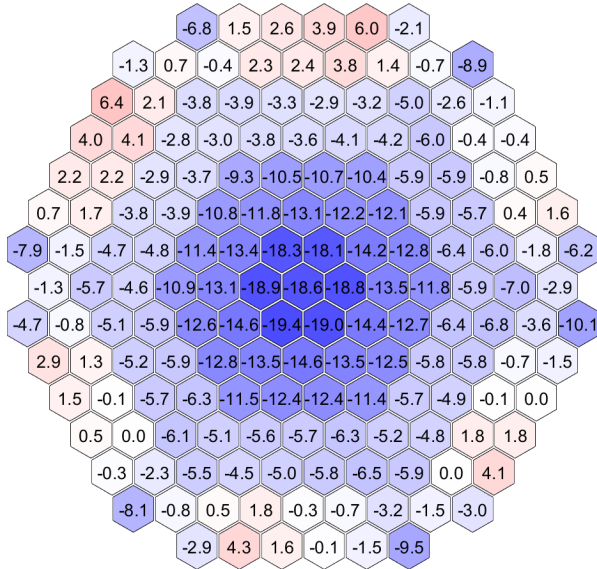


Figure 6. The relative differences in percents between the node-wise relative powers from the full core Serpent 2 calculation #1 and the HEXTRAN calculation at the axial level of the detector rods.

Most of the differences between HEXTRAN and Serpent 2 are in the middle of the core, where relative power is very small. There is a clear tilt visible in the HEXTRAN solution relative to Serpent 2 such that the relative power in the middle of the core is significantly underestimated. In the outer area where most of the relative power is located, the results are within -10.1% to +6.4% of each other. The measured significant tilt in the relative powers from the lower left of the core to the upper right was reproduced in the HEXTRAN calculation.

V. SUMMARY AND CONCLUSIONS

All full core Serpent 2 calculations and the HEXTRAN calculation overestimated the effective multiplication factor of the system. A large portion of the overestimation can be explained by the stainless steel spacers and the different Serpent 2 calculations show their effect to be -660 pcm. In addition, it is possible the experimental uncertainty of the soluble boron concentration contributes somewhat to this overestimation, as the maximum allowable concentration within the experimental accuracy produces a -577 pcm smaller effective multiplication factor.

When no spacer grid was modelled, the overestimation from Serpent 2 is in line with previous nodal diffusion results of the problem, which overestimated the effective multiplica-

tion factor by 500-1500 pcm [7]. The modelling of the spacer grids was found to be an important component in the modelling of the neutronics of the V-1000. As the group constants for HEXTRAN were generated with Serpent 2, it is likely the diffusion calculation shares some of the factors causing the overestimation with Serpent 2. However, the overestimation is significantly larger.

If the measurements from the first measure pass at the present-day NRC “Kurchatov Institute” were used, the full core Monte Carlo calculation failed to reproduce the shape of the power distribution. If the measurements from the second measurement pass were used, the Serpent 2 solution agreed with the measurements relatively well considering the sensitivity of the problem to the properties of the radial reflector. Both modelling the spacer grid and adjusting the soluble boron concentration affected the radial power distribution. The best match between Serpent 2 and measurements was obtained by modelling the spacer grids and using the highest possible soluble boron concentration within the experimental accuracy. The overestimation of the relative power of the detector rod in the assembly #100 is assumed to be a singular error as no corresponding overestimation is found in its immediate vicinity. Definite causes for the underestimations on the top-left corner of the core have not been found. The author believes the small tilt in Serpent 2 results relative to measurements are due to inaccuracies in the widths of the gaps between the assemblies and the core baffle.

The HEXTRAN results agreed with the Serpent 2 results as well as was expected. It was known from previous calculations that HEXTRAN results combined with external pin power reconstruction have roughly $\pm 10\%$ accuracy relative to measurements of the V-1000 core [7]. Therefore if the Serpent 2 calculation agrees with the measurements relatively well, Serpent 2 and HEXTRAN solutions should differ. This is in line with the obtained differences between Serpent 2 and HEXTRAN (-19.4% to +6.4%).

As the HEXTRAN code has no built-in pin power reconstruction routine, direct comparison of HEXTRAN results and measurements would not have been meaningful. If the Serpent 2 calculation agrees with the measurements relatively well, it can be used to analyse the nodal code despite the possible limitations of the case and untethered from other error sources. In this case this was underlined by the fact both the Serpent 2 and the HEXTRAN calculations produced significant overestimations in the effective multiplication factor. Considering the steep flux gradients in the core, it is possible the nodal diffusion model in HEXTRAN is unable to produce a more accurate solution relative to Serpent 2. This could be examined if the case was solved with a nodal code with a more adaptive solution scheme.

VI. ACKNOWLEDGMENTS

This work was funded by the Finnish National Research Programme on Nuclear Power Plant Safety (SAFIR2018/SADE and SAFIR2018/MONSOON).

The calculation of the V-1000 core was a more difficult task than would be obvious, as the data on the measurements

had been archived at various organizations for a relatively long time. I would like to thank the following institutions and individuals for their help in the investigations to acquire sufficiently accurate data for the calculation of the problem.

Dr. A. Kotsarev
Dr. S. Kliem
Dr. I. Panka
Dr. P.T. Petkov
Ms. H. Rätty
NRC “Kurchatov Institute”

REFERENCES

1. J. LEPPÄNEN, M. PUSA, T. VIITANEN, V. VALTAVIRTA, and T. KALTAISENAHO, “The Serpent Monte Carlo code: Status, development and applications in 2013,” *Annals of Nuclear Energy*, **82**, 142–150 (2015).
2. V. IONOV, Y. A. KRAINOV, Y. A. EPANECHNIKOV, and V. I. BARYJBKIN, “Measurements at V-1000 critical facility. Kinetics Experiments Description,” EU FP5 Report VALCO/WP3/MEAS(D3)-2, Brussels, Belgium. European Commission 5th EURATOM Framework Programme 1998-2002 (2002).
3. R. KYRKI-RAJAMÄKI, *Three-dimensional reactor dynamics code for VVER type nuclear reactors*, Ph.D. thesis, Technical Research Centre of Finland, Espoo (1995), VTT Publications 246, 51. p. + app. 80 p.
4. A. KERESZTÚRI, G. HEGYI, C. MARÁZCY, I. PANKA, M. TELBISZ, I. TROSZTEL, and C. HEGEDUS, “Development and validation of the three-dimensional dynamic code KIKO3D,” *Annals of Nuclear Energy*, **30**, 93–120 (2003).
5. U. GRUNDMANN, U. ROHDE, and S. MITTAG, “DYN3D, Three dimensional core model for steady-state and transient analysis of thermal reactors,” in “Proceedings of the PHYSOR 2000,” Pittsburgh, USA (2000), ISBN 0-89448-655-1.
6. M. P. LIZORKIN, V. N. SEMENOV, V. S. IONOV, and V. I. LEBEDEV, “Time dependent spatial neutron kinetic algorithm for BIPR8 and its verification,” in “Proceedings of the 2nd Symposium of AER,” Paks, Hungary (1992), pp. 389–407.
7. S. MITTAG, U. GRUNDMANN, F.-P. WEISS, P. T. PETKOV, E. KALOINEN, A. KERESZTÚRI, I. PANKA, A. KUCHIN, V. S. IONOV, and D. POWNEY, “Neutron-kinetic code validation against measurements in the Moscow V-1000 zero-power facility,” *Nuclear Engineering and Design*, **235**, 485–506 (2005).
8. J. I. HUTTON, “New capabilities of the WIMS code. In: Proceedings of the PHYSOR 2000,” in “Proceedings of the PHYSOR 2000,” Pittsburgh, USA (2000), ISBN 0-89448-655-1.
9. M. EDENIUS, K. EKBERG, B. H. FORSSÉN, and D. KNOTT, *CASMO-4, A fuel assembly burnup program*, Studsvik of America Inc, USA (1995), User’s Manual, STUDSVIK/SOA-95/1.
10. J. J. CASAL, R. J. J. STAMMLER, E. A. VILLARINO, and A. A. FERRI, “HELIOS: geometric capabilities of a new fuel assembly program,” in “Proceedings of the International Topical Meeting on Advances in Mathematics, Computations and Reactor Physics, vol. 2,” Pittsburgh, PA, USA (1991), pp. 10.2.1–1.
11. V. D. SIDORENKO, S. N. BOLSHAGIN, A. P. LAZARENKO, M. Y. TOMILOV, and V. M. TSVETKOV, “Spectral code TVS-M for calculation of characteristics of cells. Supercells and fuel assemblies of VVER-type reactors,” in “Proceedings of the 5th Symposium of AER,” Dobogoko, Hungary (1995), pp. 121–130, ISBN 963-372-604-2.
12. L. MAIOROV, K. ANDRZEJEWSKI, T. APOSTOLOV, R. BECKER, J. GADO, A. KERESZTÚRI, N. LALETIN, V. LEBEDEV, V. LELEK, M. LIZORKIN, M. MAKAI, A. NOVIKOV, V. PSHENIN, and M. YUDKEVICH, “Theoretical investigations of the physical properties of WWER-type uranium–water lattice,” Final Report of Temporary International Collective (TIC), vol. 2, Akadémiai Kiadó, Budapest, Hungary (1994), ISBN 963-05-6682-6.
13. P. T. PETKOV, “Development of a neutron transport code for many-group two-dimensional heterogeneous calculations by the method of characteristics,” in “Proceedings of the 10th Symposium of AER,” Moscow, Russia (2000), pp. 271–280, ISBN 963-372-622-0.
14. P. T. PETKOV, “Calculation of accurate albedo boundary conditions for three-dimensional nodal diffusion codes by the method of characteristics,” in “Proceedings of the 10th Symposium of AER,” Moscow, Russia (2000), pp. 407–417, ISBN 963-372-622-0.
15. A. KOTSAREV, Personal communication (2016).
16. R. SOITINAHO, Illustration by R. Soitinaho 10.1.2017.
17. Z. LIU, K. SMITH, and B. FORGET, “A Cumulative Migration Method for Computing Rigorous Transport Cross Sections and Diffusion Coefficients for LWR Lattices with Monte Carlo,” in “Proc. PHYSOR 2016,” Sun Valley, Idaho (May 2016).